Journal of ELECTRONIC MATERIALS, Vol. 40, No. 6, 2011
DOI: 10.1007/s11664-011-1520-5

Preparation and Properties of New Polyphenylene Sulfide/AlN Composites for Electronic Packaging

R.K. GOYAL,[1,3] P. JADHAV,[1] and A.N. TIWARI[2]

1.—Department of Metallurgy and Materials Science, College of Engineering, Pune, Shivajinagar, Pune 411 005, India. 2.—Department of Metallurgical Engineering and Materials Science, Indian Institute of Technology Bombay, Powai, Mumbai 400 076, India. 3.—e-mail: rkgoyal72@yahoo.co.in

The thermal, mechanical, and dielectric properties of new high-performance polyphenylene sulfide/aluminum nitride (AlN) composites prepared by hot pressing were investigated for use in electronic packaging. The coefficient of thermal expansion was decreased by 41%. The glass-transition temperature and Vickers microhardness were increased by 13°C and 46%, respectively, for the 15.1 vol.% AlN composite. A modified rule of mixtures with β of 0.065 fits the data. The dielectric constant and loss factor of the composites are within the range of requirements for commercial use.

Key words: Composites, glass transition, dielectric properties, microhardness, thermal expansion

INTRODUCTION

Polymer matrix composites exhibiting a unique combination of good thermal stability, high thermal conductivity, and low coefficient of thermal expansion (CTE) and dielectric constant are required for high-density wiring (HDW) or printed circuit boards (PCBs) in electronics and microelectronics.[1] In general, polymers exhibit high CTE, and low dielectric constant and thermal conductivity. Ceramics possess low CTE, and good thermal conductivity and mechanical properties. Therefore, ceramic fillers are often added to polymers to decrease the CTE and increase the thermal conductivity of the resultant composites. A number of polymer matrices such as epoxy,[2–4] cyanate ester,[5] polybenzoxazole,[6] polyimide,[7,8] polytetrafluoroethylene,[9] and polyethylene[10] reinforced with ceramic fillers have been studied. Traditionally, the most commonly used cost-effective material for PCB is epoxy resin reinforced with E-glass fibers. However, epoxy/E-glass composites have several drawbacks such as containing halogen compounds, moisture sensitivity, and poor CTE and dielectric properties, particularly at higher temperatures and frequencies.[11,12] Moreover, the highest continuous-use temperature for commercial epoxy/E-glass laminate is 130°C, and it begins to decompose at about 260°C, which is well within the typical processing temperature range of lead-free solder.[13,14] Nevertheless, industry is switching to ecofriendly lead-free electronics assembly technologies. Furthermore, epoxy composites exhibit moisture absorption of more than 2% at saturation. In plastic packages, moisture absorption above a threshold limit decreases the glass-transition temperature (T_g) and increases the dielectric constant of composites.

Hence, to combat the aforesaid drawbacks of commercial epoxy composites, high-performance polymers reinforced with thermally conducting but electrically insulating ceramic particles are required.[15,16] Polyphenylene sulfide (PPS) is a high-performance thermoplastic semicrystalline polymer which has ~65% crystallinity, good fire retardancy, and low moisture absorption. It has a high melting point (285°C to 295°C), high degradation temperature (>450°C), and good mechanical properties.[17] Its thermal, mechanical, and electrical properties could be further improved by addition of carbon nanotubes,[18,19] graphite,[20,21] $CaCO_3$,[22] clay,[23] TiO_2,[24] Al_2O_3,[25] or CuO.[26]

(Received July 24, 2010; accepted January 10, 2011; published online February 4, 2011)

However, to the best of our knowledge, until now, no results have been published on the CTE, glass-transition temperature, microhardness, and dielectric properties of aluminum nitride (AlN)-reinforced PPS composites. In the present study, AlN was used as a filler because it exhibits low intrinsic CTE (4.4×10^{-6}/°C), low dielectric constant (8.5), high thermal conductivity (230 W/m K), and good modulus (331 GPa).[27] The objective of this study is to decrease the CTE and increase the microhardness and glass-transition temperature of PPS composites reinforced with AlN particles. Such data will be useful for PCB manufacturers or engineers as they look forward to new polymer composites with properties better than those of commercial epoxy/E-glass composites. Finally, the results of the environmentally benign (i.e., halogen free with fire retardant) PPS/AlN composites fabricated by conventional hot pressing are presented and compared with data reported in the open literature.

EXPERIMENTAL PROCEDURES

Materials

PPS (M_n: 10,000) and AlN powders purchased from Aldrich Chemical Company were used in as-received condition for matrix and reinforcement, respectively. Figure 1a and b shows a typical scanning electron microscope (SEM) micrograph and differential particle size distribution of the AlN particles, respectively. The differential distribution of AlN particle size was determined using a GALAI CIS-1 laser particle size analyzer. The particle size ranged from 1.5 μm to 9.6 μm. The mean AlN particle size was 4.8 μm. As-received absolute ethanol of Merck grade was used for homogenizing the AlN and the PPS powder.

Preparation of PPS/AlN Composites

Both pure PPS and AlN powders were dried in an oven at 120°C for 3 h. The dried AlN powder was first suspended in absolute ethanol using a magnetic stirrer for 1 h. Then, PPS powder was added slowly to the AlN/ethanol suspension with concurrent stirring and heating at 80°C until dry powder was obtained. The resultant powder was further dried at 100°C for 8 h in an oven. Then, PPS/AlN composites were fabricated using hot pressing. The dried powder was filled into a tool steel die with 13 mm diameter. The powder was heated at an average heating rate of 6°C/min under a pressure of 45 MPa to a maximum temperature of 320°C. After a soaking period of 30 min, the samples were air-cooled to a temperature of 60°C, and then samples were ejected. Five different compositions containing 0 wt.%, 10 wt.%, 20 wt.%, 30 wt.%, and 50 wt.% AlN in a PPS matrix were fabricated and characterized. Table I presents the wt.% and vol.% of AlN particles added to the PPS matrix. The weight fraction of AlN can be converted to volume fraction by using the equation: $V_f = W_f/[W_f + W_m(\rho_f/\rho_m)]$, where V_f is the volume fraction, W_f is the weight fraction, and ρ_f is the density of the AlN particles. W_m and ρ_m are the weight fraction and the density of the PPS matrix, respectively.

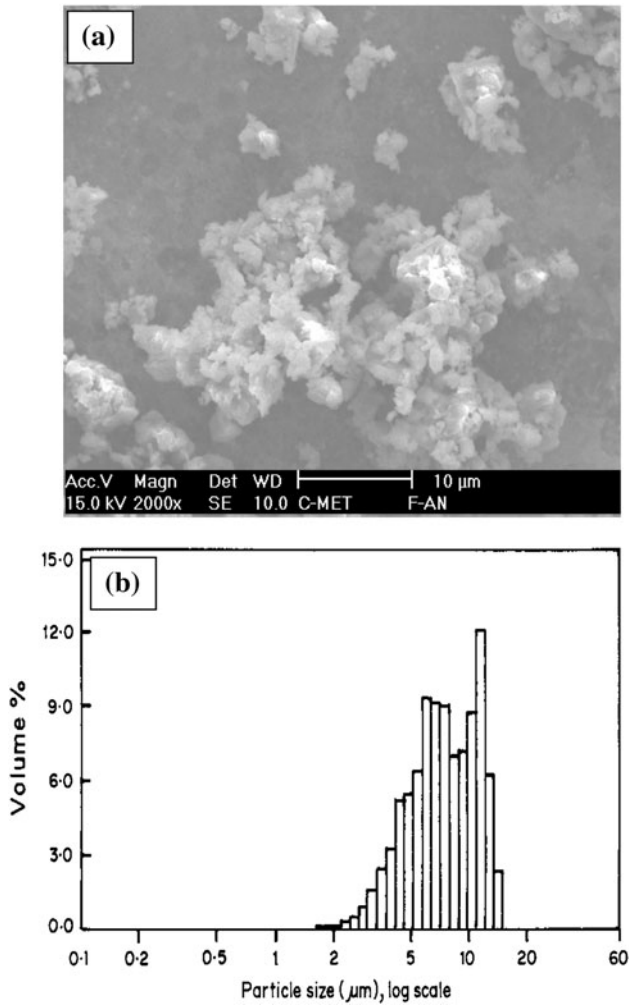

Fig. 1. (a) SEM image and (b) differential particle size distribution of AlN particles.

Table I. Wt.% and vol.% of AlN particles in the PPS matrix

	% AlN Particles in PPS Matrix	
Sample Code	**By weight**	**By volume**
PPS-0	0	0
PPS-10	10	4.9
PPS-20	20	9.4
PPS-30	30	15.1
PPS-50	50	29.3

Characterization

The theoretical density of the samples was calculated by the rule of mixture (ROM) using the density of AlN (3.26 g/cc) and of PPS (1.35 g/cc). The experimental density was measured by Archimedes' principle, where the volume was measured by buoyancy in an absolute ethanol medium. The x-ray diffraction (XRD) pattern for as-molded samples was recorded using a Philips X-Pert PANalytical PW 3040/60 to investigate the change in PPS morphology. XRD data were obtained by using Cu K_α radiation of wavelength 1.54 Å at 40 kV and 30 mA. All analyses were carried out with 2θ varying between 10° and 60° at room temperature. To study the degree of dispersion of AlN in the matrix, samples were prepared using the method described elsewhere.[1] The prepared samples were coated with platinum using a sputter coater (JEOL JEC560) and studied using SEM (JEOL JSM 6360A). The microhardness of well-polished samples was measured using a Vickers hardness tester (Future Tech Corp FM-700, Tokyo, Japan) at a constant load of 100 g and dwell time of 15 s. Average values of six readings are reported as the microhardness of the samples. The linear CTE of the annealed samples was determined using a laboratory-made dilatometer during heating from 40°C to 150°C at a heating rate of 2°C/min. The accuracy of the displacement measurement was 1 μm. The thermal strain ($\Delta L/L_0$) was plotted against the temperature, and the slope was measured. The slope between the thermal strain and the temperature is known as the linear CTE, which can be represented as: linear CTE = $\Delta L/(L_0/\Delta T)$, where ΔL is the change in length during ΔT temperature duration, and L_0 is the original length of the sample. The CTE in the temperature range of 40°C to 80°C was taken as the CTE below T_g. The meeting point of the extrapolated tangents (drawn below and above T_g) was considered the T_g of the samples. The dielectric constant was determined using a Wayne Kerr Electronics precision impedance analyzer (6515B, UK) at frequencies varying from 1 kHz to 15 MHz at 30°C. The dielectric constant (ε) was evaluated by the relation $\varepsilon = Ct/\varepsilon_0 S$, where S is the surface area and t is the thickness of the dielectric material. ε_0 is the permittivity of free space (8.854×10^{-12} F/m). The dissipation factor was obtained directly from the instrument.

RESULTS AND DISCUSSION

Density

Figure 2 shows the theoretical and experimental density of the AlN-filled PPS composites. It can be seen that the density increased with AlN loading due to the higher density of AlN (3.26 g/cc) than that of pure PPS (1.35 g/cc). The experimental density of the 5 vol.% composite was slightly higher than the theoretical density, which might be due to increased crystallinity as a result of the nucleation

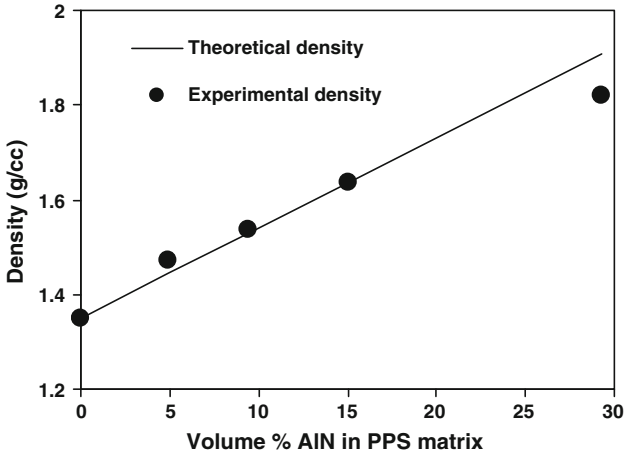

Fig. 2. Theoretical and experimental densities of PPS/AlN composites.

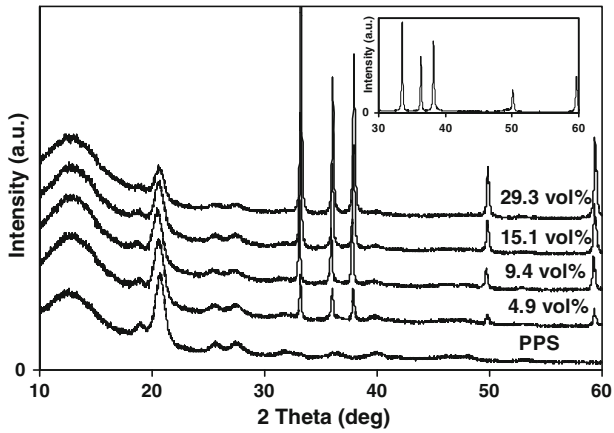

Fig. 3. XRD patterns of the PPS/AlN composites. For clarity, the scans for the 4.9 vol.%, 9.4 vol.%, 15.1 vol.%, and 29.3 vol.% AlN composites are displaced upwards by 1000, 2000, 3000, and 4000, respectively.

effect of AlN particles.[16] These results confirm that the samples are almost void free up to 15.1 vol.% AlN content. However, thereafter, the density of the composites deviated downwards compared with the theoretical values, which may be due to the presence of voids in the samples; for example, the 29.3 vol.% composite had voids of 5.2%. Increasing the vol.% of AlN in the matrix leads to a decrease in interparticle distances, and thus aggregation of particles. These aggregates hinder the infiltration of the highly viscous polymer, which results in voids in the samples at higher particle loading.

X-Ray Diffraction

The diffraction peak positions (2θ) of the major crystallographic reflections for the PPS composites are shown in Fig. 3. Pure PPS and the PPS constituent of the composites crystallize with an orthorhombic crystal structure. The 2θ value for pure PPS was observed at 19.01°, 20.99°, 25.77°,

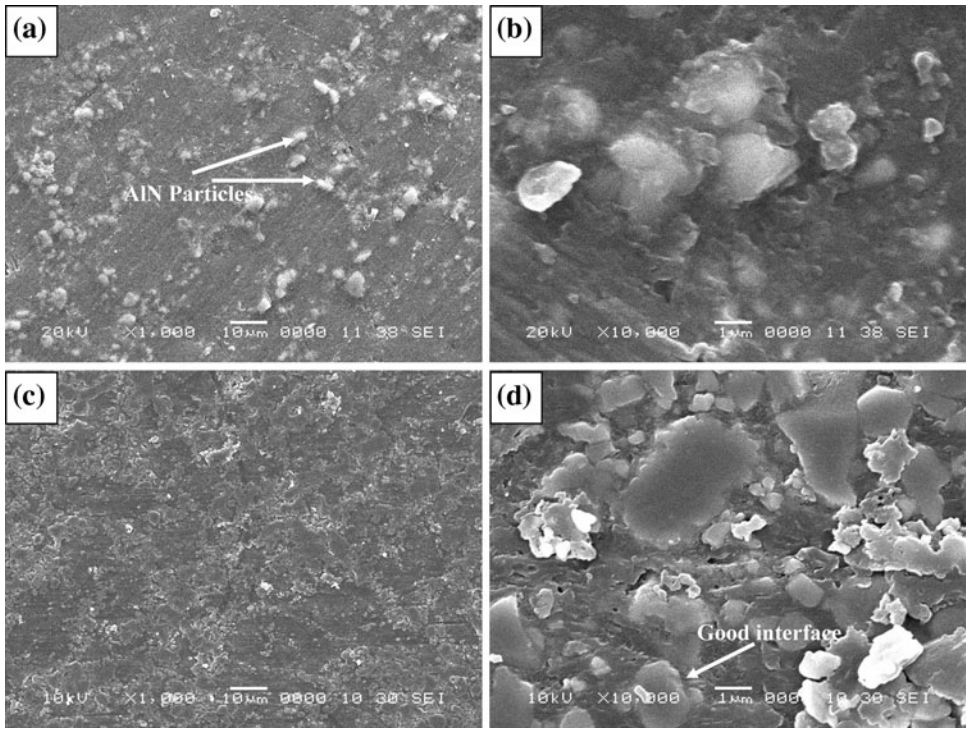

Fig. 4. SEM images of polished PPS composites containing: (a, b) 15.1 vol.% AlN and (c, d) 29.3 vol.% AlN; scale bar: 10 μm (a, c) and 1 μm (b, d).

and 28.19°, corresponding to diffraction planes of 110, 111, 112, and 211, respectively. For the AlN-filled PPS composites, some additional AlN peaks were also observed at 33.19°, 36.08°, 37.92°, 49.81°, and 59.3°, corresponding to diffraction planes of 100, 002, 101, 102, and 110 of hexagonal AlN, respectively. However, new diffraction peaks were not observed for the composites, indicating that there was no change in the morphology of the PPS. For some of the polymer composites, a new diffracting peak was observed, which implies a new crystal structure of the polymer.[28] The intensity of both constituents varies in proportion to their loading; for example, the intensity of AlN peaks increases with increasing AlN content.

Scanning Electron Microscopy

Figure 4 shows SEM images of the polished specimens of the PPS composites. Figure 4a and c are SEM images of the 15.1 vol.% and 29.3 vol.% AlN-filled PPS composites, respectively, at 1000× magnification. It can be seen that the AlN particles are distributed uniformly. However, some aggregates consisting of a few primary AlN particles are observed in the 29.3 vol.% composite. Figure 4b and d show that the AlN particles are well coated with PPS matrix and there is no distinct boundary between the AlN particles and the PPS matrix. This might be because of good adhesion between them. The interparticle distances are quite low in the 29.3 vol.% composite compared with the 15.1 vol.% composite. Due to the decrease in interparticle distances, a larger number of aggregates are observed in Fig. 4d. Moreover, some voids of submicron size are also observed, which might be the reason for the decreased density of the 29.3 vol.% composite.

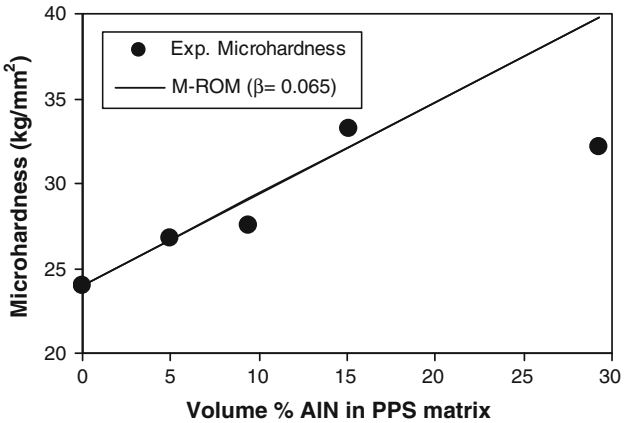

Fig. 5. Vickers microhardness of the PPS/AlN composites.

Vickers Microhardness

Figure 5 shows the microhardness of the composites as a function of AlN content. The microhardness increases with increasing AlN content, due to the resistance to plastic deformation of the PPS matrix contributed by the hard AlN particles. The microhardness of the 15.1 vol.% and 29.3 vol.%

composites increased from 24 kg/mm^2 for the pure PPS matrix to 33 kg/mm^2 and 32 kg/mm^2, respectively. The lower hardness of the 29.3 vol.% composite than that of the 15.1 vol.% composite may be attributed to the presence of voids, as confirmed by density and SEM analysis. Composite microhardness has been correlated with the values predicted from a modified ROM:[29] $H_c = \beta \cdot H_f \cdot V_f + H_m \cdot V_m$, where H_c, H_f, and H_m are the microhardness of the composite, the AlN particles, and the PPS matrix, respectively. β is the strengthening efficiency factor, which depends on the aspect ratio and distribution of the reinforcements in the PPS matrix. The value of β for randomly distributed glass fiber is 0.2.[30] This value can be extended to less than 0.2 for a particle-reinforced polymer composite. A value of β of 0.065 fits the data well up to 15.1 vol.% AlN content. This is in good agreement with the β value of 0.065 for polyetheretherketone (PEEK)/AlN composites.[29]

Coefficients of Thermal Expansion

The linear thermal strain ($\Delta L/L_0$) for pure PPS and the 29.3 vol.% composite is shown in Fig. 6. The expansion is due to the fact that there is movement of molecules or segments as they get energy with increasing temperature. The thermal strain of the 29.3 vol.% composite is lower than that of pure PPS; for example, the thermal strain for pure PPS during heating from 40°C to 150°C is 0.82%, whereas for the 29.3 vol.% composite it is decreased to 0.59%. This is due to the constraints imposed by the microsized, irregularly shaped AlN particles on the mobility of the polymer chains.[31,32] The glass-transition temperature (T_g) was considered as the meeting point of tangents extrapolated from curves of thermal strain versus temperature. T_g increases with increasing AlN content, i.e., from 84°C for pure PPS to 97°C for the 15.1 vol.% composite, as shown in Fig. 7. This is due to the hindrance of mobility of the polymer chains. However, an insignificant increase in T_g was observed thereafter because of the formation of AlN aggregates.

The out-of-plane linear CTE of the composites is plotted as a function of AlN content in Fig. 8. It can be seen that the CTE of pure PPS is 52 × 10^{-6}/°C. The CTE of the composites decreased significantly with increasing AlN content. Compared with pure PPS, the CTE for the 15.1 vol.% and 29.3 vol.% composites was decreased by 33% and 41%, i.e., to 34.8 × 10^{-6}/°C and 30.6 × 10^{-6}/°C, respectively. The CTE of the 29.3 vol.% composite is close to that of copper. This is apparently due to the constraint imposed on the polymer chain mobility. Figure 8 also shows the correlation between the experimental CTEs and the values predicted by the ROM. The ROM overestimated the CTEs, as it does not take into account the interaction between the particles and the PPS matrix.[32] Presently, commercial glass/epoxy (FR-4) composite is used as a packaging substrate in electronics, having a much higher out-of-plane CTE (>60 × 10^{-6}/°C) than that of copper (18 × 10^{-6}/°C).[33] The CTE of copper must match that of the packaging substrate material to avoid

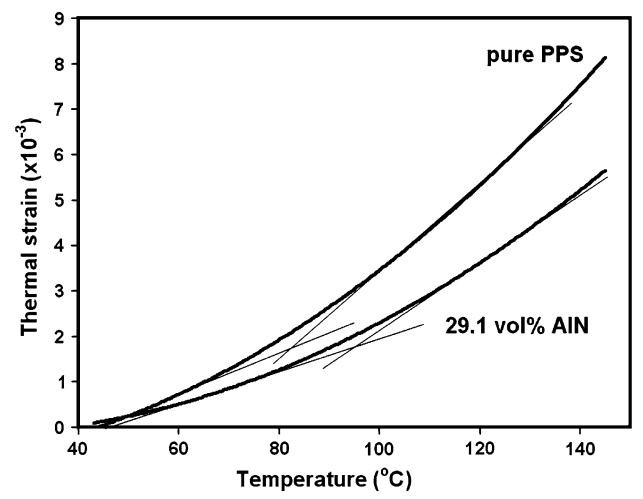

Fig. 6. Thermal strain ($\Delta L/L$) of the composites as a function of temperature (40°C to 140°C).

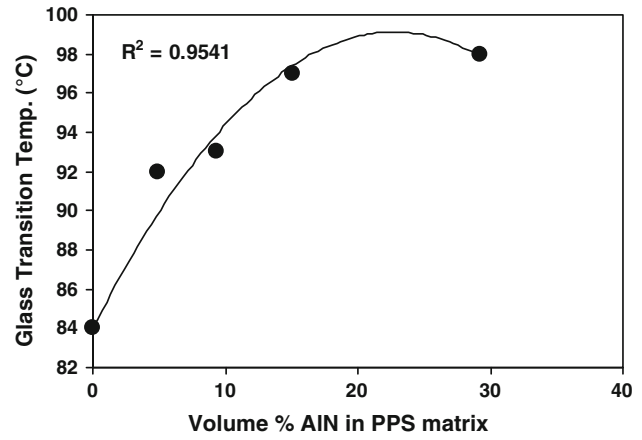

Fig. 7. Glass-transition temperature (T_g) of the PPS/AlN composites.

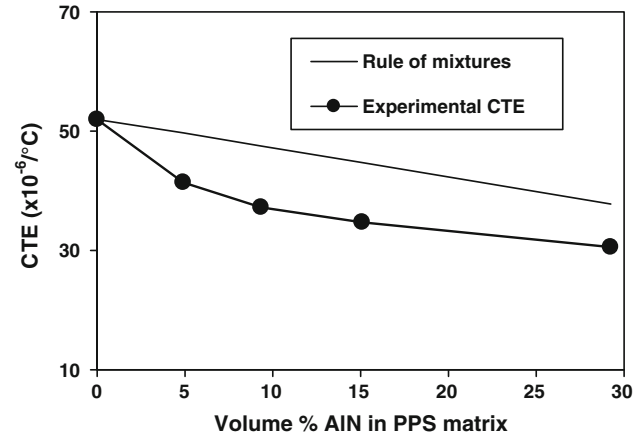

Fig. 8. Experimental and theoretical linear CTE of the composites.

thermal fatigue failure. In the present work, the decrease in CTE with increasing AlN content indicates better dimensional stability of the composites as compared with pure PPS, making them potential candidate electronic packaging materials.

Dielectric Properties

Figure 9a and b show the dielectric constant of the PPS/AlN composites as a function of the logarithm of frequency and AlN content, respectively. It can be seen clearly from Fig. 9a that the dielectric constant of the composites is weakly frequency dependent from 10 kHz to 15 MHz. However, below 10 kHz, it is slightly higher because of Maxwell–Wagner polarization at the interfaces between the filler and the PPS matrix. A similar trend in dielectric constant was investigated for AlN-filled[7] and modified zirconia-filled[34] polyimide composites. Figure 9a shows the dielectric constant for the pure PPS and the composites measured at 1 MHz. The dielectric constant of pure PPS is 3.25. It can be seen from Fig. 9b that the dielectric constant of the composites increased with increasing AlN content. The dielectric constant of the 15.1 vol.% and 29.3 vol.% composites is 4.53 and 4.3, respectively. The increased dielectric constants are due to the greater polarization of the AlN than that of the PPS matrix. In the case of the 29.3 vol.% composite, the dielectric constant is smaller than that of the 15.1 vol.% composite. This is due to the presence of voids, as confirmed by the density and SEM studies. The dielectric constant of air is 1, and hence, the effective dielectric constant of the composites with higher AlN loading decreases. The dissipation factor (tan δ) measured at 1 MHz for pure PPS was 0.004. It varied in the range of 0.014 to 0.020 for the composites, with no trends with increasing AlN content. Similar to this, the dissipation factor for 50 vol.% AlN-filled polyimide increased to 0.020 compared with pure polyimide (0.002 at 100 kHz).[7] A comparison of the properties of PPS/AlN composites with that of commercial epoxy/E-glass laminate is shown in Table II. It can be clearly seen that the thermal and dielectric properties of the PPS/AlN composites are comparable to those of the commercial product, and hence, these composites may be useful materials in the future for electronic packaging substrates. It is to be noted that these composites have inherent fire-retardant properties. In contrast to this, commercial epoxy-based laminates show fire retardancy due to the presence of bromine compounds. Moreover, the thermal stability of the PPS matrix composites is greater[18] than that of epoxy-based composites/laminates.[13,14]

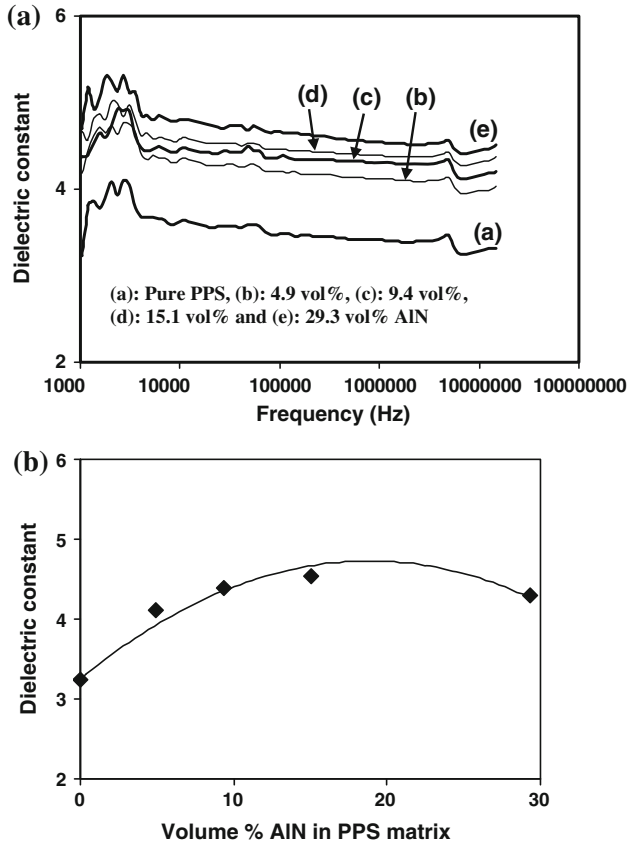

Fig. 9. Dielectric constant of composites versus (a) frequency and (b) vol.% AlN.

CONCLUSIONS

High-performance PPS matrix composites reinforced with 0 vol.% to 29.3 vol.% (50 wt.%) AlN particles were successfully fabricated by hot pressing. The microhardness was increased from 24 kg/mm^2 for pure PPS to 33.2 kg/mm^2 for the 15.1 vol.%

Table II. Properties of PPS/AlN and commercial FR-4 epoxy/glass composite

Materials	Density (g/cc)	T_g (°C)	CTE ($\times 10^{-6}$/°C)	Microhardness (kg/mm^2)	Dielectric Constant (1 MHz)	tan δ (1 MHz)	References
Pure PPS	1.35	84	52	24	3.25	0.004	Exp.[a]
PPS/AlN (15.1 vol.%)	1.636	97	34.8	33.2	4.53	0.018	Exp.[a]
FR-4 epoxy/glass	1.80	125–135	60	–	4.7	0.02	11,33

[a]Experimental result.

composite, and thereafter, it decreased due to the presence of voids. The linear CTE of the composites was decreased by up to 41%. The glass-transition temperature (T_g) was increased by 13°C for the 15.1 vol.% composite. The improvement in CTE and T_g was attributed to the decrease in polymer chain mobility and a decrease in free volume of the PPS matrix. The dielectric constant increased to 4.5, and there was weak frequency dispersion. Both dielectric constant and dissipation factor are comparable to those of a commercial product. Therefore, based on these results, it can be suggested that such PPS/AlN composite materials may be suitable for electronic packaging applications.

ACKNOWLEDGEMENTS

P.J. and R.K.G. are thankful to Professor N.K. Nath and Professor S.P. Butee, Department of Metallurgy and Materials Science, College of Engineering, Pune for their suggestions.

REFERENCES

1. R.K. Goyal, A.N. Tiwari, U.P. Mulik, and Y.S. Negi, *Compos. Sci. Technol.* 67, 1802 (2007).
2. C.P. Wong and S.B. Raja, *J. Appl. Polym. Sci.* 74, 3396 (1999).
3. M. Chaturvedi and Y.-L. Shen, *Acta Mater.* 46, 4287 (1998).
4. W. Kim, J.-W. Bae, I.-D. Choi, and Y.-S. Kim, *Polym. Eng. Sci.* 39, 756 (1999).
5. T.J. Wooster, S. Abrol, J.M. Hey, and D.R. MacFarlane, *Composites A* 35, 75 (2004).
6. H. Ishida and S. Rimdusit, *Thermochem. Acta* 320, 177 (1998).
7. L. Li and D.D.L. Chung, *J. Electron. Mater.* 23, 557 (1994).
8. K.E. Gonsalves, X. Chen, and M.-I. Baraton, *Nanostruct. Mater.* 9, 181 (1997).
9. W.C.-Y. Yui, C.W. Chen, Y.Z. Wu, and Y.-C. Chen, *Electrochem. Solid State Lett.* 8, F1 (2005).
10. J. Gu, Q. Zhang, J. Dang, J. Zhang, and Z. Yang, *Polym. Eng. Sci.* 49, 1030 (2009).
11. *Electronic Materials Handbook, Packaging*, vol. 1 (Materials Park: ASM International Handbook Committee, 1998).
12. M. Iji and Y. Kiuchi, *J. Mater. Sci.: Mater. Electron.* 15, 175 (2004).
13. Datasheet of Polyclad Laminates, Inc. www.becker-mueller.de, 2004.
14. Datasheet of Sanmina-SCI Corp. www.sanmina-sci.com, 2005.
15. N.C. Frederic, ed., *Thermoplastic Aromatic Polymer Composites* (Oxford: Butterworth Heinemann Ltd., 1992).
16. R.K. Goyal (Ph.D. thesis, Indian Institute of Technology Bombay, Mumbai, 2007).
17. J. Mark, ed., *Polymer Data Handbook* (London: Oxford University Press, 1999).
18. S. Yu, W.M. Wong, Y.K. Juay, and M.S. Yong, *SIMTech Technical Rep.* 8, 71 (2007).
19. J. Yang, T. Xu, A. Lu, Q. Zhang, H. Tan, and Q. Fu, *Compos. Sci. Technol.* 69, 147 (2009).
20. Y.F. Zhao, M. Xiao, S.J. Wang, X.C. Ge, and Y.Z. Meng, *Compos. Sci. Technol.* 67, 2528 (2007).
21. R.K. Goyal, S.D. Samant, A.K. Thakar, and A. Kadam, *J. Phys. D* 43, 365404 (2010).
22. X. Wang, W. Tong, W. Li, H. Huang, J. Yang, and G. Li, *Polym. Bull.* 57, 953 (2006).
23. H. Zou, W. Xu, Q. Zhang, and Q. Fu, *J. Appl. Polym. Sci.* 99, 1724 (2006).
24. Z. Jiang, L.A. Gyurova, A.K. Schlarb, K. Friedrich, and Z. Zhang, *Compos. Sci. Technol.* 68, 734 (2008).
25. M.H. Cho, S. Bahadur, and A.K. Pogosian, *Wear* 258, 1825 (2005).
26. S. Bahadur and C. Sunkara, *Wear* 258, 1411 (2005).
27. L.M. Sheppard, *Ceram. Bull.* 69, 1801 (1990).
28. L. Priya and J.P. Jog, *J. Polym. Sci. B* 40, 1682 (2002).
29. R.K. Goyal, A.N. Tiwari, and Y.S. Negi, *Mater. Sci. Eng. A* 491, 230 (2008).
30. T.H. Farebrother and J.A. Raymond, *Polymer Engineering Composites*, ed. M.O.W. Richardson (London: Applied Science, 1977), pp. 197–235.
31. G. Tsagaropoulos and A. Eisenberg, *Macromolecules* 28, 6067 (1995).
32. R.K. Goyal, A.N. Tiwari, U.P. Mulik, and Y.S. Negi, *J. Phys. D* 41, 085403 (2008).
33. R.T. Rao, J.R. Eugene, and G.K. Alan, *Microelectronics Packaging Handbook, Technology Drivers, Part I*, 2nd ed. (London: Chapman and Hall, 1997).
34. S.-F. Wang, Y.-R. Wang, K.-C. Cheng, J.-H. Chen, and Y.-P. Hsaio, *J. Electron. Mater.* 37, 925 (2008).